Catalysis Today 151 (2010) 39–45

Contents lists available at ScienceDirect

Catalysis Today

journal homepage: www.elsevier.com/locate/cattod

Aqueous photocatalytic oxidation of amoxicillin

D. Klauson [a,*], J. Babkina [a,1], K. Stepanova [a,1], M. Krichevskaya [a,1], S. Preis [b]

[a] Department of Chemical Engineering, Tallinn University of Technology, Ehitajate tee 5, 19086 Tallinn, Estonia
[b] Department of Chemical Engineering, Lappeenranta University of Technology, P.O. Box 20, 53851 Lappeenranta, Finland

ARTICLE INFO

Article history:
Available online 10 February 2010

Keywords:
Photocatalytic oxidation
Amoxicillin
Doped titania
Reaction pathway

ABSTRACT

Aqueous photocatalytic oxidation (PCO) of amoxicillin (AMO), a β-lactam antibiotic, was experimentally studied. Degussa P25 titanium dioxide and visible light-sensitive sol–gel synthesized carbon- and iron-doped titania were used as photocatalysts. The efficiency of PCO dependent on initial AMO concentration and pH was established. A number of organic and inorganic by-products were determined allowing construction of a possible reaction pathway.

1. Introduction

For the last years the interest towards the fate of medicines, especially antibiotics, has been arising. Being refractory substances [1–3], antibiotics pass the biological treatment plants intact [4], either remaining in the liquid phase or, dependent on their hydrophilicity, adsorbing to the active sludge with subsequent desorption to the environment [5]. These substances in the environment are potent in the damage of micro-flora and fauna, accumulate in food chains [6,7], and accelerate the development of resistant micro-organisms, including pathogens [8–11]. The accumulation of antibiotics in organisms may cause arthropathy, nephropathy, damages in central nervous system and spermatogenesis, mutagenic effects and light sensitivity [2].

One of the most widely used antibiotics is amoxicillin (AMO, (2*S*, 5R, 6R)-6-{[(2*R*)-2-amino-2-(4-hydroxyphenyl)-acetyl]amino}-3,3-dimethyl-7-oxo-4-thia-1-azabicyclo[3.2.0] heptane-2-carboxylic acid, see Fig. 1), a moderate-spectrum bacteriolytic β-lactam antibiotic. There are only a few works dealing with the advanced oxidation processes (AOPs) application to the AMO degradation: Fenton oxidation [12–14] and photocatalytic oxidation (PCO) with Fluka anatase [15]. The elucidation of the AMO PCO reaction pathway makes the novelty of the present research, since the published works on the AOPs of antibiotics mainly focus on the parent compound removal and mineralization, leaving the degradation by-products unexplored.

Photocatalytic oxidation is one of AOPs based on the action of positively charged holes on the surface of illuminated semiconductor, most often titanium dioxide. Water molecules decompose on the holes to form powerful hydroxyl radicals [16]; the hole itself also can degrade the pollutant having even higher oxidation potential [17]. The electrons, excited by the UV-irradiation, also participate in the PCO, reducing dissolved oxygen resulting in the formation of other radical oxidants. The ratio of radical to hole oxidation reactions depends on the properties of the substance to be degraded. Many substances may be degraded by both mechanisms simultaneously, e.g. [18–20].

Although commercial photocatalysts, such as Degussa P25 titanium dioxide, exhibit a good performance, they can use only a small ultraviolet fraction (4%) of solar radiation reaching the earth surface due to the high energy of its band-gap [21]. This makes sensitising TiO_2-based photocatalysts to visible light the potential way of widening of utilised solar spectrum. For this purpose, titanium dioxide can be doped with various metals or non-metals, which can effectively reduce the band-gap [22–28] for excitation of electrons by lower energy photons at greater wavelength up to 540 nm as reported. However, the authors found earlier that the doped titania photocatalysts may, unlike "universal" P25, oxidise only selected pollutants [29]. This can be explained by the smaller redox potential and, possibly, faster electron–hole recombination of the catalysts with smaller band-gap [30].

2. Materials and methods

Two thermostatted at 20 ± 1 °C 200-ml batch reactors with inner diameter 100 mm (evaporation dishes), irradiated contact surface 40 m^2/m^3, agitated with magnetic stirrers, were used in PCO experiments: the one used for the PCO was called "active" and the

---

[*] Corresponding author. Tel.: +372 620 2857; fax: +372 620 2856.
E-mail address: deniss.klauson@ttu.ee (D. Klauson).
[1] Tel.: +372 620 2857; fax: +372 620 2856.

0920-5861/$ – see front matter © 2010 Elsevier B.V. All rights reserved.
doi:10.1016/j.cattod.2010.01.015

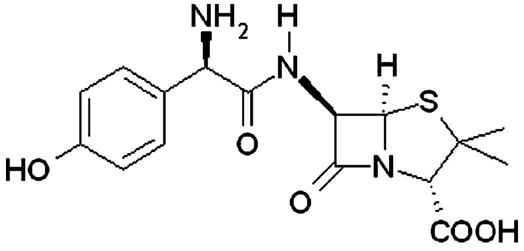

Fig. 1. Amoxicillin (AMO) molecule.

other containing no photocatalyst was called “reference”. Both reactors were exposed to the identical experimental conditions. The samples from the active reactor were compared to the reference samples to avoid complications caused by water evaporation. An artificial UV-light source, Phillips 365-nm low pressure luminescent mercury UV-lamp (15 W), was positioned horizontally over the reactors, providing the irradiance of about 0.5 mW/cm^2 measured at a distance corresponding to the level of the surface of the reactor by the optical radiometer Micropulse MP100 (Micropulse Technology, UK). With artificial daylight fluorescent lamp (Phillips TL-D 15W/33-640), the irradiance could not be directly measured. The illuminance was measured using TES 1332 luxmeter (TES Inc., Taiwan) reaching 3700 lx (lm/m^2), which corresponds to the irradiance of 0.6 mW/cm^2. The irradiance was calculated using lumen to watt ratio of 684, as the response of the human eye to the illuminance of 684 lm equals to that to the irradiance of 1 W [31]. With AMO PCO experiments were conducted outdoors using natural solar radiation; the irradiance was measured by luxmeter approximating 16 mW/cm^2.

Titanium dioxide was used as 1 g/l slurry. The experiments were carried out with aqueous solutions of AMO supplied by Sigma–Aldrich. In the experiments, the initial concentration of AMO varied between 1 and 100 mg/l. The influence of the initial pH was studied in the range from 3 to 9, adjusted by 4N sulphuric acid or 15% sodium hydroxide. At pH higher than 9 the slurry became stable with no chance to separate it by centrifugation or filtration, making the measurements impossible. The pH was monitored throughout the experiments without adjustment. The treatment time was chosen to be 6 h under artificial light of the UV and vis lamps, and 2 h under natural solar radiation: the results in conversion degrees are reported for these times.

All the experiments were carried out for at least three times under identical experimental conditions. The average deviation of data in parallel experiments did not exceed 5%.

Amoxicillin concentration was determined photometrically, using the light absorbance at 230 nm, using Helios β spectrophotometer. Chemical oxygen demand (COD) was determined by a standard dichromate method [32], using HACH kits LCK 314 (15–150 mg O/l) and LCK 414 (5–60 mg O/l). The concentration of ammonium ion was determined photometrically using a modified version of a standard phenate method [32]. Nitrate and sulphate anions were determined using Metrohm 761 Compact IC ionic chromatograph. A Waters Aquity UPLC combined with MS and quadrupole-time of flight (Q-TOF) mass-analyzer was used for the determination of organic AMO PCO by-products. An Aquity UPLC BEH C_{18} 1.7 μm 2.1 mm × 100 mm column was used, with water and 0.1% formic acid as eluent A (initial eluent) and acetonitrile with 0.1% formic acid as eluent B. The complete change from eluent A to B was achieved in 15 min out of 20 min run with linear gradient used. Mass spectra were acquired in a full scan mode (50–500 amu). The instrument was operated in positive ion mode, with capillary voltage of 2400 V. The mass spectrometry data was handled using MassLynx software.

The accuracy of UV-absorbance in AMO concentration measurements was checked by the parallel determination of AMO in MS analysis of the PCO-treated samples with the AMO preconstructed calibration curves for both methods: the difference observed between AMO concentrations determined by UV-absorbance and MS did not exceed 2% at highest, suggesting negligible amounts of UV-absorbance by PCO by-products. For this reason, the UV-absorbance was used as a simpler and less time- and resource-consuming approach than MS. It was noted that the UV-absorbance spectra of PCO-treated solutions did not exhibit a change in shape, showing no new peaks or a wavelength shift in maximum absorbance. Poor accumulation of UV-absorbing PCO by-products may be explained by their oxidation rates being comparable to or exceeding those of AMO. A similar analytical approach has been used in oxidation studies with other antibiotics of aromatic structure, such as sulphamethazine [33], chloramphenicol [11], and flumequine [34].

Adsorption experiments were carried out in closed thermostatted flasks equipped with magnetic stirrers at 20 ± 1 °C. The amount of adsorbed substance was derived from the batch mass balance: the concentration of the dissolved substance was determined before and after adsorption. The adsorption equilibrium was experimentally determined to be reached in 6 h. In order to determine AMO concentration in the adsorption experiments, the UV-absorbance was used.

Six specimens of carbon-doped titania were obtained by the hydrolysis of tetrabutyl orthotitanate at room temperature without adjustment of pH being around 5.5–6.0, followed by drying and calcination at different temperatures (200–700 °C). Five iron-doped titania catalysts with calculated iron content from 0.42 to 3 at.% were prepared by the pulverisation of 75 ml of tetrabutyl orthotitanate into 1 l pre-sonicated Fe_2O_3 suspensions of various concentrations (0.1–0.7 g/l); the hydrolysis was followed by sonication, drying and calcination at 200 °C. After calcinations, all the catalysts were washed with hot (70–80 °C) distilled water applied in a sequence of 10–15 rinsing rounds (ca. 1 l per 1 g of catalyst) in order to clean the catalyst surface from water-soluble compounds.

The crystallinity of carbon-doped titania was analyzed using D5000 Kristalloflex, Siemens (Cu-Kα irradiation source) X-ray diffraction spectroscope (XRD). Carbon content was measured with PHI 5600 X-ray photoelectron spectroscope. The specific area (BET and Langmuir adsorption) and the pore volume of the catalysts were measured by the adsorption of nitrogen using KELVIN 1042 sorptometer.

3. Results and discussion

3.1. PCO experiments with Degussa P25

The results of AMO PCO were expressed in its concentration decrease rate and the PCO efficiency, E, defined as the decrease in the amount of the pollutant divided by the amount of energy reaching the surface of the treated sample. The efficiency is calculated according to the following equation [35]:

$$E = \frac{\Delta c \times V \times 1000}{I \times S \times t} \qquad (1)$$

where E, PCO efficiency, mg/(W h); Δc, the decrease in the pollutant's concentration, mg/l, or COD, mg O/l; V, the volume of the sample to be treated, l (in this case, 0.2 l); I, irradiance, mW/cm^2; S, irradiated area, cm^2; t, treatment time, h.

The best performance was observed at pH 6.0, occurring naturally in the AMO solutions, followed by alkaline and acidic media. The dependence of AMO conversion x on its initial concentration from 1 to 100 mg/l may be seen in Fig. 2. The increase in conversion at smaller concentrations reaches its peak at approximately 10–25 mg/l (dependent on pH), and is followed by a

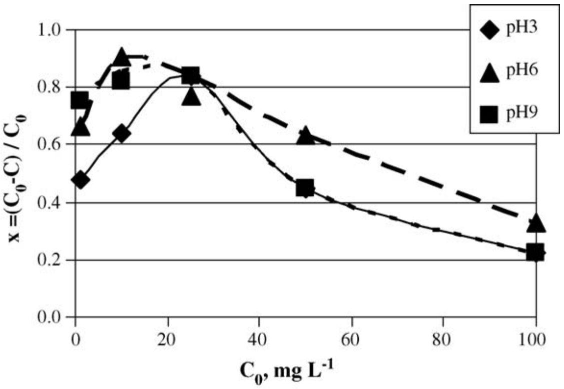

Fig. 2. The dependence of AMO conversion on its initial concentration: artificial UV, 20 °C, treatment time 6 h.

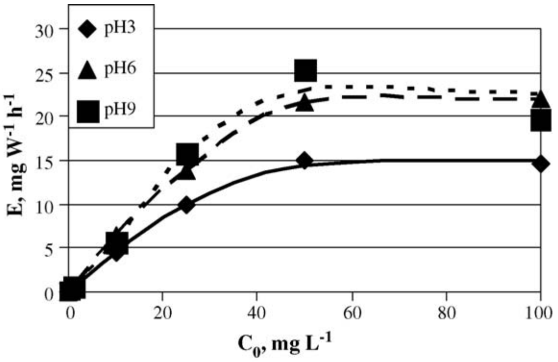

Fig. 3. The dependence of PCO efficiency on the AMO initial concentration: 20 °C.

swift decrease, which may be explained by changes in reaction rate control mechanism: the reaction rate limitation at smaller concentrations, when the active sites on the catalyst surface are only partially occupied by adsorbed AMO molecules, changes to the mass transfer limitation, when all the active sites on the photocatalyst surface are filled at higher AMO concentrations, and a new AMO molecule can be adsorbed only after desorption or complete oxidation of the degradation by-products. Thus, above 20–25 mg/l PCO efficiency and, subsequently, the absolute amount of degraded AMO (see Eq. (1)) remains constant, as one can see from Fig. 3. In the majority of the experiments, COD decrease was between 10 and 40%.

The addition of *tert*-butyl alcohol (TBA) as a radical scavenger to the solution to be treated in the amount equimolar with AMO (0.068 mM, i.e. 25 mg/l of AMO and 5 mg/l of TBA) did not alter the latter's degradation rate, which allows suggesting the dominance of hole reactions: the radical oxidation should be noticeably affected by the presence of TBA.

Since the radical reactions appeared to play a minor role in the PCO of AMO, the adsorption of the latter on the catalyst surface attracted an interest as a relevant circumstance: the behaviour of the oxidation efficiency consistent with the adsorption may support the hypothesis of the hole oxidation. The adsorption of AMO on TiO_2 was observed to be rather low increasing with concentration growth up to 3.5 mg/g (ca. 0.009 mmol/g) at the AMO concentration of about 100 mg/l. Judging from the PCO results fitting well to the Langmuir–Hinshelwood description (Section 3.1, Figs. 2 and 3), the adsorption of AMO fits well to the PCO performance: in the studied concentration range, the adsorption of AMO on the Degussa P25 may be adequately described by both Langmuir ($R^2 = 0.9538$) and Freundlich ($R^2 = 0.9912$) equations (Eqs. (2) and (3)), derived from the adsorption experiments data:

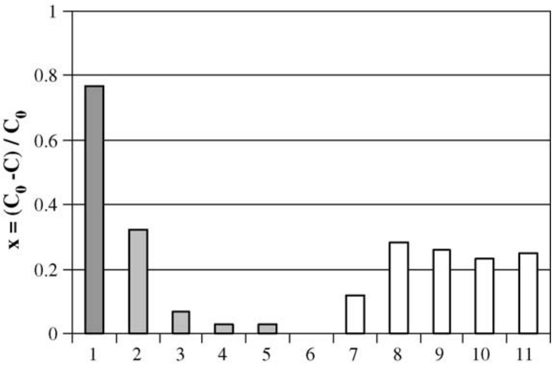

Fig. 4. AMO degradation degree at doped catalysts with visible light in 6-h treatment: 1, P25 with UV; 2, 37 at.% C, 200 °C; 3, 34.9 at.% C, 400 °C; 4, 34.9 at.% C, 500 °C; 5, 30.4 at.% C, 600 °C; 6, 34.7 at.% C, 700 °C; 7, 0.42 at.% Fe; 8, 0.89 at.% Fe; 9, 1.33 at.% Fe; 10, 2.2 at.% Fe; 11, 3.0 at.% Fe; all Fe–TiO_2 samples calcinated at 200 °C; AMO 25 mg/l; pH 6.0.

$$q_L = 0.011 \times \frac{15.979 \times c}{1 + 15.979 \times c} \quad (2)$$

$$q_{Fr} = 0.0145 \times c^{0.3437} \quad (3)$$

where AMO adsorption q is in mmol/g, and its concentration c is in mM.

3.2. PCO experiments with carbon- and iron-doped titania

The parameters of carbon-doped catalysts can be seen in Table 1. Under artificial visible light these catalysts showed AMO conversion around 30% at 25 mg/l (pH 6.0), whereas Degussa P25 under UV of similar intensity showed almost 80%. The best catalytic performance was achieved with the highest carbon content. AMO conversion decreased significantly with decreasing carbon content (see Fig. 4). The AMO conversion degree with iron-doped titania increased from 12 to 25% with iron content growing from 0.42 to 0.89 at.% (Fig. 4), remaining more or less unchanged with increasing iron content. The COD decrease was with doped catalysts around 10–30%. Adsorption experiments were also undertaken with doped titania samples. They showed very low

Table 1
The parameters of carbon-doped titania photocatalysts.

Calcination *T*, °C	Crystallographic composition, %			Composition, at.%			S_{BET}, m^2/g	$S_{Langmuir}$, m^2/g	Micropore area, m^2/g	Micropore volume, mm^3/g
	Anatase	Brookite	Rutile	Ti	O	C				
200	71.9	28.1	–	17.2	45.8	37.0	202.3	278.9	0	0
400	78.1	21.9	–	18.1	46.6	34.9	105.7	144.7	4.12	1.54
500	76.9	18.2	5.0	18.5	46.6	34.9	39.45	53.85	3.95	1.39
600	74.4	25.6	–	20.0	49.6	30.4	8.81	12.08	0	0
700	–	–	100	18.0	47.3	34.7	3.52	4.81	0.20	0.07

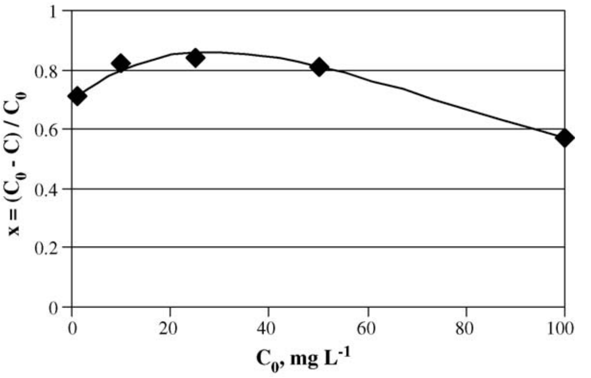

Fig. 5. AMO conversion vs. its initial concentration with Degussa P25 under solar radiation: pH 6.0, 20 °C, treatment time 2 h.

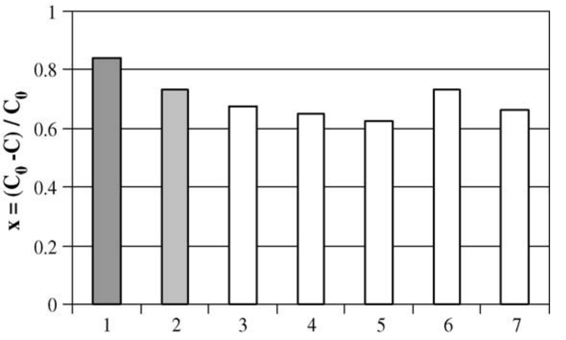

Fig. 6. AMO degradation degree at doped catalysts with solar light in 2-h treatment: 1, P25; 2, 37 at.% C; 3, 0.42 at.% Fe; 4, 0.89 at.% Fe; 5, 1.33 at.% Fe; 6, 2.2 at.% Fe; 7, 3.0 at.% Fe; AMO 25 mg/l, pH 6.0.

adsorption of AMO on their surface not exceeding the limits of analytical precision.

3.3. Solar PCO experiments

Amoxicillin degradation with Degussa P25 under solar radiation proceeded about three times faster than under artificial UV (Fig. 5). Since carbon-doped catalysts showed insufficient performance, only the most effective catalyst with the highest carbon content (37 at.% C, 200 °C) and iron-doped photocatalysts were used in solar PCO experiments, with which the AMO degradation proceeded also faster than with artificial light: the performance of doped catalysts was moderately inferior to that of P25 (Fig. 6). The disproportional improvement of oxidation rates, about three times for Degussa P25 and about seven times for the doped catalysts, may be explained by the difference in the irradiance with UV and visible light in solar spectrum: the intensity of radiation in solar spectrum grows dramatically with increasing wavelength from 300 to 500 nm, whereas the experiments with lamps were carried out under similar irradiance conditions.

3.4. Amoxicillin PCO by-products and reaction pathway

Ammonia, nitrate and sulphate were detected in small amounts as the AMO PCO inorganic products indicating the most of nitrogen and sulphur remaining in organic by-products: nitrogen mineralized to 1.5% and sulphur to 14% extent. The COD reduction was also observed to be within 10–30% thus making the mineralization idea offered. A number of organic by-products were determined qualitatively using UPLC coupled with ESI-MS. The degradation by-products were determined for AMO concentration ranges

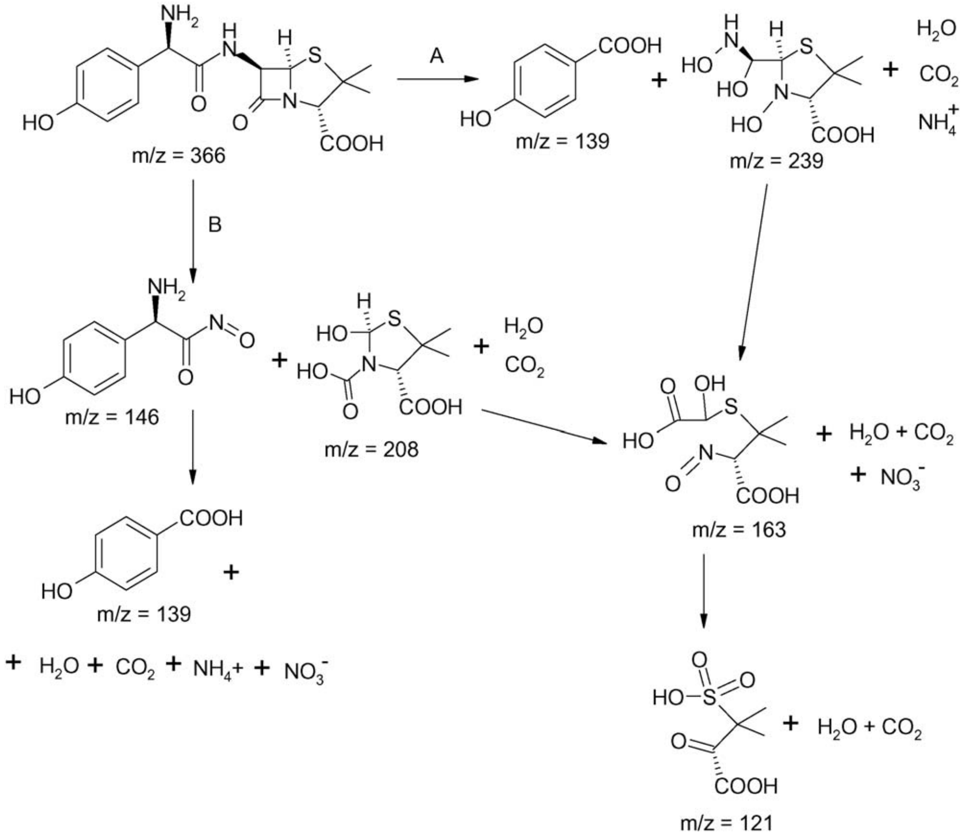

Fig. 7. PCO reaction pathway at AMO concentration of 10 mg/l (kinetic reaction rate control): pH 6.0, 20 °C.

corresponding with the different reaction rate controlling phenomena: reaction kinetics at 10 mg/l, transitional rate at 25 mg/l and mass transfer at 100 mg/l at starting pH 6.0. The organic by-products identified were somewhat different in those cases, although some were common for all the concentrations.

Judging from the identified by-products, the following reaction pathways for AMO PCO may be proposed. Under kinetics rate control at 10 mg/l (Fig. 7), the reaction has two clearly observable pathways, where AMO molecule is cleaved initially with the release of *p*-hydroxybenzoic acid (*m*/*z* = 139, pathway A) or of a more complex compound (*m*/*z* = 146, pathway B), with its subsequent degradation to a product with *m*/*z* = 121. In transitional reaction at 25 mg/l (Fig. 8), also, two separate reaction pathways may be proposed. The first one (Fig. 8, A) is initiated by AMO molecule fragmentation at the peptide bond that is closer to the aromatic cycle, forming *p*-hydroxybenzoic acid (*m*/*z* = 139) and a bicyclical lactamic product with *m*/*z* = 160. The latter is subsequently degraded into an open-chain structure (*m*/*z* = 114), which was the ultimate AMO PCO by-product detected in this instance. The other pathway (Fig. 8, B) begins with the destruction of lactamic bond and is then followed by the destruction of the same peptide bond as in the first stage of pathway A. In the mass transfer-controlled reaction at 100 mg/l (Fig. 9), there are four possible reaction pathways detected: the first one (Fig. 9, A) is initiated by the AMO molecule cleavage, whereas the other one (Fig. 9, B) appears to begin with the break-away of the primary amino group and its subsequent replacement with the oxygen atom (*m*/*z* = 365). The pathway C is similar to A, however, the lactamic group remains intact after the initial molecule break-up. Pathway D is initiated by the hydroxylation of the aromatic cycle. Interesting is the increased number of different reaction pathways in the mass transfer-controlled reaction: since the AMO molecules

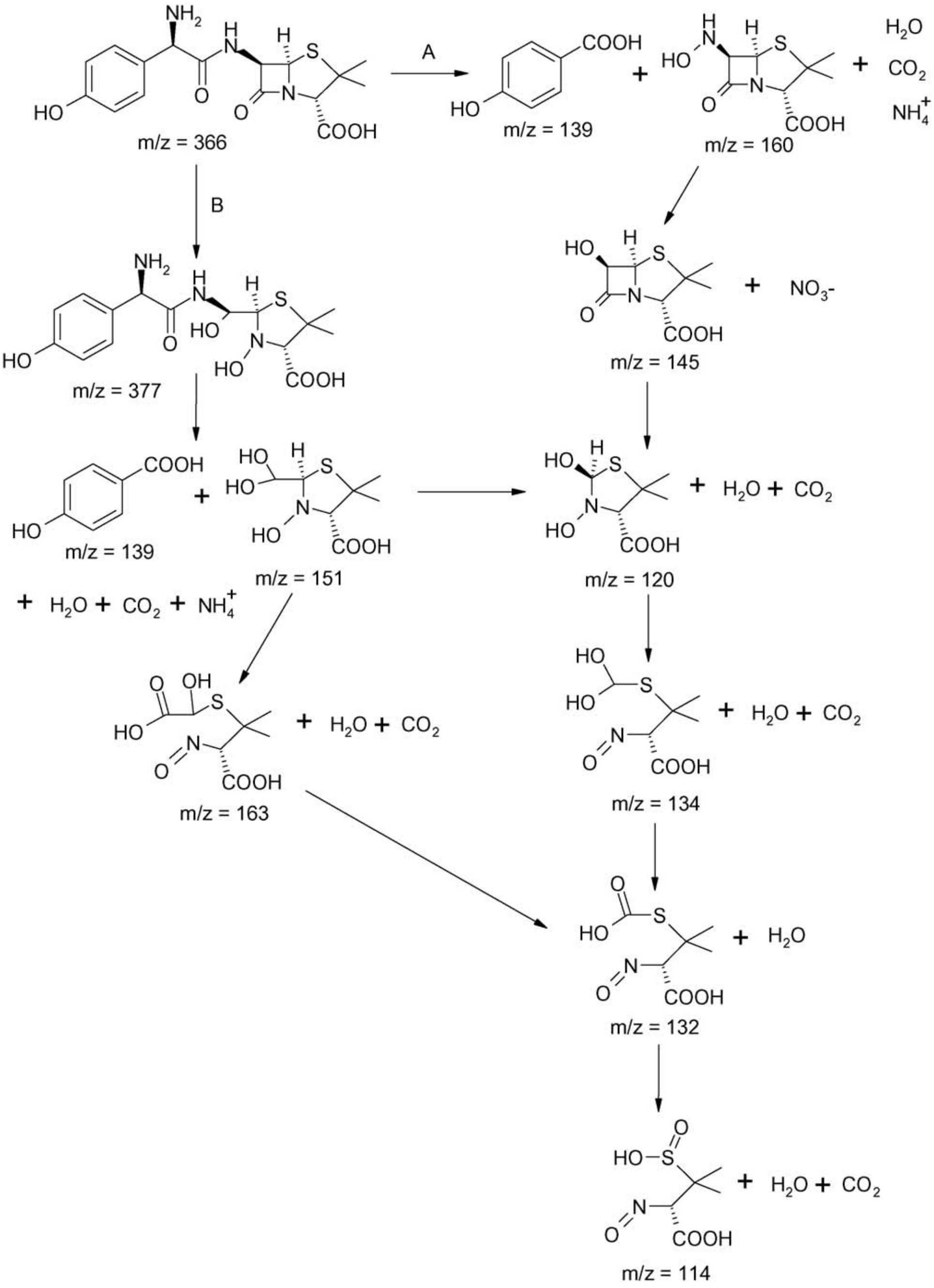

Fig. 8. PCO reaction pathway at AMO concentration of 25 mg/l (transition reaction rate control): pH 6.0, 20 °C.

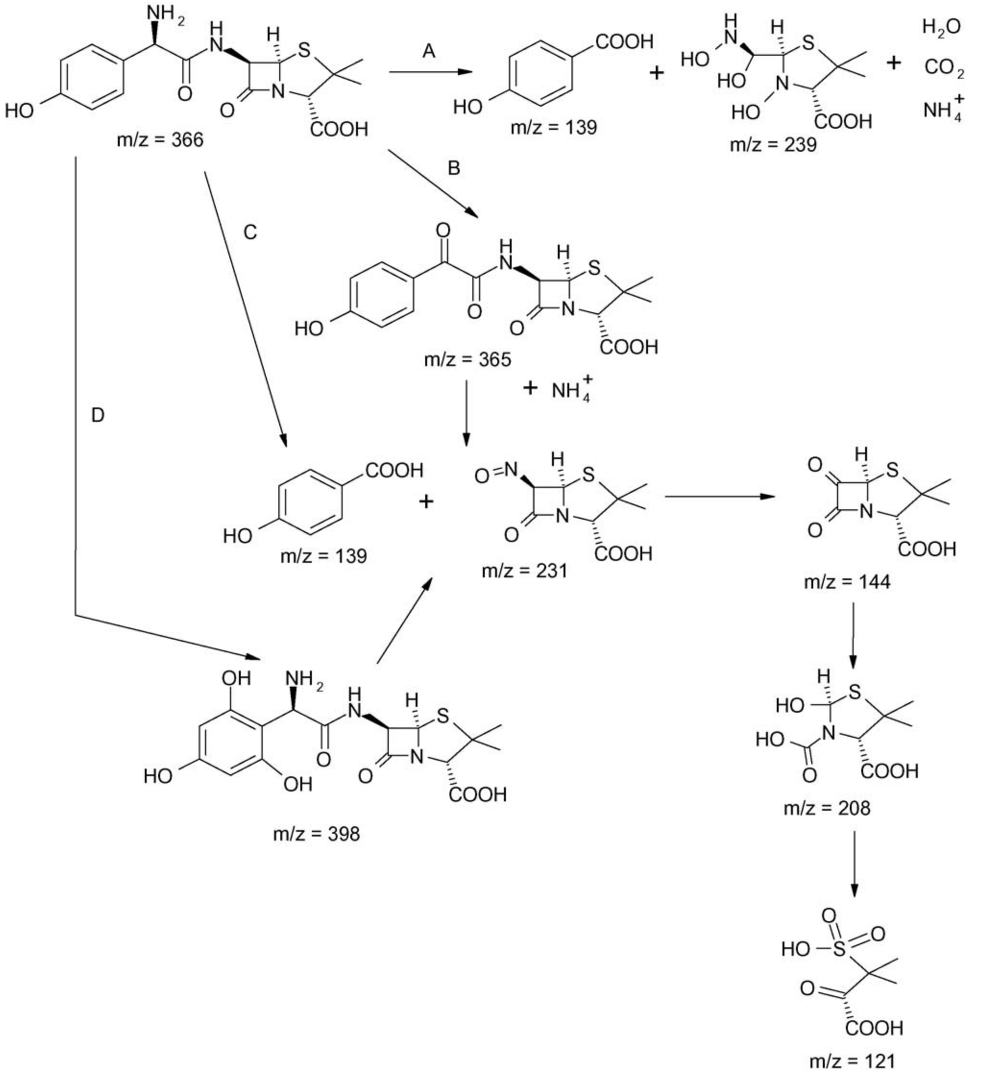

Fig. 9. PCO reaction pathway at AMO concentration of 100 mg/l (mass transfer reaction rate control): pH 6.0, 20 °C.

compete to adsorb on active sites on the surface, steric obstacles from the neighbouring AMO molecules lead to their adsorption by various functional groups, hence resulting in wider diversity of PCO reaction products and pathways.

4. Conclusions

Aqueous photocatalytic oxidation (PCO) of a widely used β-lactam antibiotic, amoxicillin (AMO) was studied using Degussa P25 titanium dioxide and visible light-sensitive synthetic sol–gel titania catalysts doped with carbon and iron. Although yielding to P25 under artificial light, doped catalysts were close by their efficiency to Degussa catalyst under solar radiation. The PCO of AMO proceeds with maximum efficiency in neutral solutions. The PCO efficiency increases with growing concentration of AMO achieving maximum at 50 mg/l and remaining constant with further concentration increase. The PCO products, determined under various AMO concentration conditions, allow the suggestion of possible reaction pathways.

Acknowledgements

The authors would like to thank Mr. Petri-Jaan Lahtvee and Ms. Liisa Arike, Competence Centre of Food and Fermentation Technology, for their help in UPLC-MS analyses, Dr. Mai Uibu, Laboratory of Inorganic Materials, Tallinn University of Technology, for the measurements of the photocatalysts' surface area, the team of Prof. Dr.-Ing. Joachim Deubener, Division of Glass and Glass Technology, Institute of Nonmetallic Materials of the Technical University of Clausthal and especially Dr. Anna Moiseev for providing XRD measurements, Mr. Andrew S. Cavanaugh, the University of Colorado at Boulder, for providing XPS measurements. The authors express their gratitude to the Estonian Science Foundation (grant 7541), and the United States Civilian Research and Development Foundation (grant US16062) for financial support of the research.

References

[1] A. Al-Ahmad, F.D. Daschner, K. Kümmerer, Biodegradability of cefotiam, ciprofloxacin, meropenem, penicillin G, and sulfamethoxazole and inhibition of wastewater bacteria, Arch. Environ. Contam. Toxicol. 37 (1999) 158–163.
[2] K. Kümmerer, A. Al-Ahmad, V. Mersch-Sundermann, Biodegradability of some antibiotics, elimination of their genotoxicity and affection of wastewater bacteria in a simple test, Chemosphere 40 (2000) 701–710.
[3] R. Alexy, T. Kümpel, K. Kümmerer, Assessment of degradation of 18 antibiotics in the Closed Bottle Test, Chemosphere 57 (2004) 505–512.
[4] T. Herberer, Occurrence, fate, and removal of pharmaceutical residues in the aquatic environment: a review of recent research data, Toxicol. Lett. 131 (2002) 5–17.

[5] M.N. Abellan, B. Bayarri, G. Gimenez, J. Costa, Photocatalytic degradation of sulfamethoxazole in aqueous suspension of TiO_2, Appl. Catal. B 74 (2007) 233–241.
[6] B. Halling-Sørensen, S. Nors Nielsen, P.F. Lanzky, F. Ingerslev, H.C. Holten Lützhoft, S.E. Jørgensen, Occurrence, fate and effects of pharmaceutical substances in the environment—a review, Chemosphere 36 (1998) 357–393.
[7] C. Hartig, T. Storm, M. Jekel, Detection and identification of sulphonamide drugs in municipal waste water by liquid chromatography coupled with electrospray ionisation mass spectrometry, J. Chromatogr. A 845 (1999) 163–173.
[8] S. Kim, P. Eichhorn, J.N. Jensen, A.S. Weber, D.S. Aga, Removal of antibiotics in wastewater: effect of hydraulic and solid retention times on the fate of tetracycline in the activated sludge process, Environ. Sci. Technol. 39 (2005) 5816–5823.
[9] W. Baran, J. Sochacka, W. Wardas, Toxicity and biodegradability of sulfonamides and products of their photocatalytic degradation in aqueous solutions, Chemosphere 65 (2006) 1295–1299.
[10] H. Sørum, in: F.M. Aarestrup (Ed.), Antimicrobial Resistance in Bacteria of Animal Origin, American Society for Microbiology Press, Washington, DC, 2006.
[11] A. Chatzikakis, C. Berberidou, I. Paspaltsis, G. Kyriakou, T. Sklaviadis, I. Poulios, Photocatalytic degradation and drug activity reduction of Chloramphenicol, Water Res. 42 (2008) 386–394.
[12] E.S. Emolla, M. Chaudhuri, Degradation of the antibiotics amoxicillin, ampicillin and cloxacillin in aqueous solutions by the photo-Fenton process, J. Hazard. Mater. 172 (2009) 1476–1481.
[13] C. Mavronikola, M. Demetriou, E. Hapeshi, D. Partassides, C. Michael, D. Mantzavinos, D. Kassinos, Mineralisation of the antibiotic amoxicillin in pure and surface waters by artificial UVA- and sunlight-induced Fenton oxidation, J. Chem. Technol. Biotechnol. 84 (2009) 1211–1217.
[14] A.G. Trovó, S.A. Santos Melo, R.F. Pupo Nogueira, Photodegradation of the pharmaceuticals amoxicillin, bezafibrate and paracetamol by the photo-Fenton process—application to sewage treatment plant effluent, J. Photochem. Photobiol. A 198 (2008) 215–220.
[15] E.S. Elmolla, M. Chaudhuri, Photocatalytic degradation of amoxicillin, ampicillin and cloxacillin antibiotics in aqueous solutions using UV/TiO_2 and UV/H_2O_2/TiO_2 photocatalysis, Desalination, 252 (2010) 46-52.
[16] B. Sun, M. Seto, J.S. Clements, Optical study of active species produced by a pulsed corona discharge in water, J. Electrostat. 39 (1997) 189–202.
[17] D. Bahnemann, Photocatalytic water treatment: solar energy applications, Sol. Energy 77 (2004) 445–459.
[18] R.W. Matthews, Photo-oxidation of organic material in aqueous suspensions of titanium dioxide, Water Res. 20 (1986) 569–578.
[19] V. Brezova, Š. Vodny, M. Vesely, M. Ceppan, L. Lapcik, Photocatalytic oxidation of 2-ethoxyethanol in a water suspension of titanium dioxide, J. Photochem. Photobiol. A 56 (1991) 125–134.
[20] J. Chen, D.F. Ollis, W.H. Rulkens, H. Bruning, Photocatalysed oxidation of alcohols and organochlorides in the presence of native TiO_2 and metallized TiO_2 suspensions. Part II: photocatalytic mechanisms, Water Res. 33 (1999) 669–676.
[21] Y. Zhang, J.C. Crittenden, D.W. Hand, D.L. Perram, Fixed-bed photocatalysts for solar decontamination of water, Environ. Sci. Technol. 28 (1994) 435–442.
[22] C. Lettmann, K. Hildenbrand, H. Kisch, W. Macyk, W.H. Maier, Visible light photodegradation of 4-chlorophenol with a coke-containing titanium dioxide photocatalyst, Appl. Catal. B 32 (2001) 215–227.
[23] E. Arpac, F. Sayilkan, M. Asiltürk, P. Tatar, N. Kiraz, H. Sayilkan, Photocatalytic performance of Sn-doped and undoped TiO_2 nanostructured thin films under UV and vis-lights, J. Hazard. Mater. 140 (2007) 69–74.
[24] T. Ihara, M. Miyoshi, Y. Iriyama, O. Matsumoto, S. Sugihara, Visible-light active titanium dioxide realized by an oxygen-deficient structure and by nitrogen doping, Appl. Catal. B 42 (2003) 403–409.
[25] S.D. Sharma, D. Singh, K.K. Saini, C. Kant, V. Sharma, S.C. Jain, C.P. Sharma, Sol–gel-derived super-hydrophilic nickel doped TiO_2 film as active photo-catalyst, Appl. Catal. A 314 (2006) 40–46.
[26] D. Li, H. Haneda, Sh. Hishita, N. Ohashi, Visible-light-driven nitrogen-doped TiO_2 photocatalysts: effect of nitrogen precursors on their photocatalysis for decomposition of gas-phase organic pollutants, Mater. Sci. Eng. B 117 (2005) 67–75.
[27] Z. Wang, W. Cai, X. Hong, X. Zhao, F. Xu, C. Cai, Photocatalytic degradation of phenol in aqueous nitrogen-doped TiO_2 suspensions with various light sources, Appl. Catal. B 57 (2005) 223–231.
[28] T. Ohno, M. Akiyoshi, T. Umebayashi, K. Asai, T. Mitsu, M. Matsumura, Preparation of S-doped TiO_2 photocatalysts and their photocatalytic activities under visible light, Appl. Catal. A 265 (2004) 115–121.
[29] D. Klauson, S. Preis, Visible light-assisted aqueous photocatalytic oxidation of organic pollutants using nitrogen-doped titania, Environ. Chem. Lett. 6 (2008) 35–39.
[30] Z. Liu, D.D. Sun, P. Guo, J.O. Leckie, One-step fabrication and high photocatalytic activity of porous TiO_2 hollow aggregates by using a low-temperature hydrothermal method without templates, Chem. Eur. J. 13 (2007) 1851–1855.
[31] S.J. Kirkpatrick, A primer on radiometry, Dent. Mater. 21 (2005) 21–26.
[32] L.S. Clesceri, A.E. Greenberg, R.R. Trussel, Standard Methods for the Examination of Water and Wastewater, 17th ed., APHA, AWWA, WPCF, Washington, DC, 1989
[33] S. Kaniou, K. Pitarakis, I. Barlagianni, I. Poulios, Photocatalytic oxidation of sulfamethazine, Chemosphere 60 (2005) 372–380.
[34] R. Palominos, J. Freer, M.A. Mondaca, H.D. Mansilla, Evidence for hole participation during the photocatalytic oxidation of the antibiotic flumequine, J. Photochem. Photobiol. A 193 (2008) 139–145.
[35] S. Preis, M. Krichevskaya, Y. Terentyeva, A. Moiseev, J. Kallas, Treatment of phenolic and aromatic amino compounds in polluted waters by photocatalytical oxidation, J. Adv. Oxid. Technol. 5 (2002) 77–84.